JOURNAL OF COMPUTATIONAL PHYSICS 53, 513–523 (1984)

Note

Application of a Log-Linear Element to a Finite-Element Boundary-Layer Flow Model*

1. INTRODUCTION

Numerical modeling of boundary-layer flows is made difficult because of the large cross-stream gradients in streamwise velocity near the boundary. Taylor and Delage [1] have pointed out the inaccuracies that can occur in finite-difference schemes for such models unless (1) a special wall layer is assumed, or (2) extremely small grid spacings are used near the boundary. Finite-element models of boundary-layer flow that use conventional linear or quadratic elements have similar difficulties in resolving the flow.

We have developed a class of boundary elements for use in modeling geophysical flows with the finite-element method, especially atmospheric flow in the earth's planetary boundary layer. These elements have both logarithmic and linear terms for the vertical direction and a quadratic function in the streamwise direction. These functional forms permit more accurate representation of the logarithmic velocity profile normal to the boundary and also allow for future applications to flow over irregular terrain, which will be approximated by the quadratic streamwise terms. The log-linear elements also are used to interpolate the temperature profile in the vertical direction for simulations of nonneutral flow. Applications to the atmospheric boundary layer show significantly improved accuracy over conventional quadratic elements and permit much larger time steps to be used because of the much coarser grid permitted.

2. LOG-LINEAR ELEMENT

In an attempt to address the problem of large gradients of streamwise velocity in turbulent boundary layer flow, Taylor, Hughes, and Morgan [2] incorporated a special logarithmic wall element into their finite-element model for pipe flow. Their 8-node wall element (in 2-D) was formulated to incorporate a no-slip boundary condition. They were able to reduce the number of elements by about a factor of 2 without loss of accuracy by use of the logarithmic element.

* Journal Paper No. J-10751, Iowa Agriculture and Home Economics Experiment Station, Ames, Iowa 50011, Project No. 2521.

0021-9991/84 $3.00

More recently, Hutton [3] and Hutton and Smith [4] have reported log-linear and "quadralog" wall elements for use in the simulation of duct flows having both laminar and turbulent regions. Their approach has been to position the wall element a small distance away from the surface and use a slip boundary condition, thereby avoiding the linear velocity region next to the wall. Their elements use normal derivatives of velocity in addition to velocity as nodal parameters at nodes closest to the wall.

Geophysical flows, such as the flow of the earth's atmospheric boundary layer, share similarities with pipe and duct flow, in that large cross-stream gradients of streamwise velocity result from the effect of the boundary. In contrast to the engineering flow, atmospheric problems seldom specify the conditions of the earth's surface in such detail that a laminar sublayer is applicable. Rather, the characteristics of the surface are approximated by specifying a "surface roughness" z_0, which modulates the resulting velocity profile under neutral flow,

$$\bar{u} = \frac{u_*}{k} \ln\left(\frac{z}{z_0}\right), \tag{1}$$

where $\bar{u}$ is the time-averaged horizontal velocity at height z, k is von Karman's constant, and $u_* = |\tau_s|^{1/2}$ is the "friction velocity," which is determined from the surface stress. It is, therefore, customary to have $\bar{u} = 0$ at z_0 as the lower boundary condition for atmospheric boundary-layer models.

In the presence of diabatic cooling the atmospheric velocity is observed to acquire a linear modification of the logarithmic shape described empirically [5] by

$$\bar{u} = \frac{u_*}{k}\left(\ln\frac{z}{z_0} + 4.7\zeta\right), \tag{2}$$

where $\zeta = z/L$, L being the Monin–Obhukov length ($L \to \infty$ for neutral flow, $L \to 1$ for typical nighttime cooling). If the surface is heated, the empirical velocity profile is more complex, but for weak heating, the departure from logarithmic dependence is linear.

These observations suggest that a log-linear boundary element would be appropriate for a finite-element model of the atmospheric boundary-layer velocity. Because our previous boundary-layer modeling [6] has employed 9-node elements for velocity, we chose to add a special boundary element to our element library that had the same nodal configuration as our previously used elements. The resulting boundary element has 9 nodes, with quadratic variation in the streamwise direction and log-linear variation in the vertical direction as shown in Fig. 1. The velocity approximation then is given by

$$\bar{u} = a(\xi)\ln\left(\frac{1+\Delta+\eta}{\Delta}\right) + b(\xi)\left(\frac{1+\Delta+\eta}{\Delta}\right) + c(\xi), \tag{3}$$

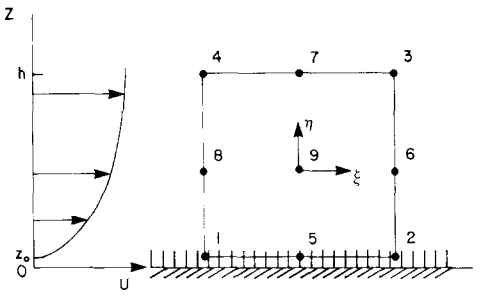

FIG. 1. Nine-node element that has log-linear terms for interpolating vertical variation of temperature and streamwise velocity.

where a, b, and c contain the streamwise quadratic behavior, and Δ depends on z_0/h, where h is the physical height of the boundary element. We found that $\Delta = 3.5z_0/h$ worked very well. Shape functions used for the interpolation are given in the Appendix. These shape functions have the desirable property [7] that their sum is unity anywhere in the boundary element.

Integration of the diffusion term for the special boundary element requires the evaluation of

$$\int \frac{\partial \bar{u}}{\partial z} K_z \frac{\partial \bar{u}}{\partial z} dz \sim \int \frac{1}{z} dz, \tag{4}$$

where the $1/z$ dependence results because K_z is proportional to z. Conventional Gauss quadrature, even tenth order, gave unsatisfactory numerical integration of this term because of the contribution from near z_0. We have employed a scheme that integrates $1/z$ exactly with 3 points (to be consistent with our 3-point Gauss quadrature in nonboundary elements). All other terms are integrated using standard 3-point Gauss quadrature. The computational time for integrations over the log-linear element therefore is comparable with that required for the quadratic elements.

We have tested the log-linear element against a conventional quadratic (9-node) element in a one-dimensional time-dependent simulation of diffusion-dominated flow of 50 m depth (similar to that observed in the lowest 50 m of the atmosphere under isothermal conditions) over a surface of assumed roughness parameter z_0 equal to 0.01 m, with diffusivity given by $K = ku*(z - z_0)$. We specify $u*$ as 0.35 m/s. The flow is driven by an imposed velocity at 50 m, and $u(z_0) = 0$. (Coriolis forces have been ignored for this test.)

For comparison with the conventional method of resolving the boundary-layer flow, we have constructed two grids to span the 50-m depth with 6 and 10 quadratic elements whose sizes are logarithmically increasing away from the boundary. A linear velocity profile was used as an initial condition.

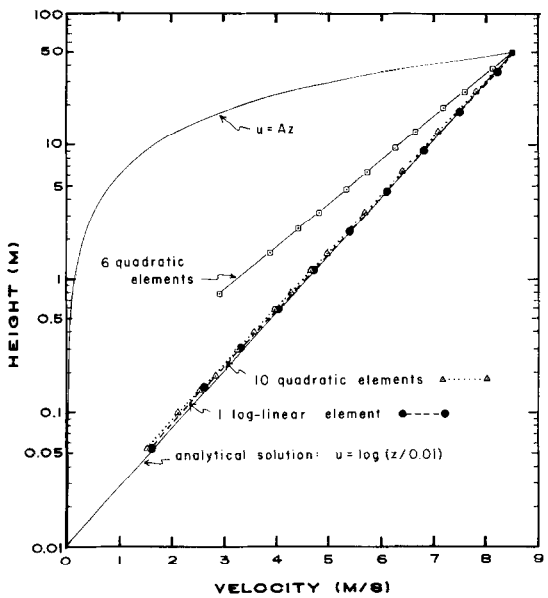

FIG. 2. Numerically generated velocity profiles for domains of 6 quadratic elements, 10 quadratic elements, and 1 log-linear element compared to the analytic solution for diffusivity given by $K = ku_*(z - z_0)$ and $z_0 = 0.01$ m.

Figure 2 shows the result of these three simulations compared with the analytic solution. The single log-linear element result is clearly more accurate than even the 10-element simulation that uses quadratic elements. The 10-element quadratic grid has 19 free nodes, the lowest of which is at 0.054 m, whereas the log-linear element has one free node at 25 m and thus has a minimum Δz 460 times larger than the 10-element grid. Therefore, in addition to superior accuracy, the log-linear element has a diffusion-stability time-step limit for explicit schemes that is significantly larger than that for the fine-resolution quadratic mesh.

3. Application to an Atmospheric Model

We have incorporated the log-linear element into the element library of our atmospheric boundary-layer model. This model is an extension of the hydrostatic model developed by Chan, Gresho, and Lee [8] which uses the hydrostatic Boussinesq equations

X momentum:
$$\frac{\partial \bar{u}}{\partial t} + \bar{u}\frac{\partial \bar{u}}{\partial x} + \bar{w}\frac{\partial \bar{u}}{\partial z} - \frac{\partial}{\partial x}\left(K_x^m \frac{\partial \bar{u}}{\partial x}\right) - \frac{\partial}{\partial z}\left(K_z^m \frac{\partial \bar{u}}{\partial z}\right) = \Theta \frac{\partial \bar{\pi}}{\partial x} - f(V_g - \bar{v}), \tag{5}$$

Y momentum:
$$\frac{\partial \bar{v}}{\partial t} + \bar{u}\frac{\partial \bar{v}}{\partial x} + \bar{w}\frac{\partial \bar{v}}{\partial z} - \frac{\partial}{\partial x}\left(K_x^m \frac{\partial \bar{v}}{\partial x}\right) - \frac{\partial}{\partial z}\left(K_z^m \frac{\partial \bar{v}}{\partial z}\right) = f(U_g - \bar{u}), \tag{6}$$

Z momentum:
$$\frac{\partial \bar{\pi}}{\partial z} = \frac{g}{\Theta^2}\bar{\theta}, \tag{7}$$

Thermodynamic energy:
$$\frac{\partial \bar{\theta}}{\partial t} + \bar{u}\frac{\partial \bar{\theta}}{\partial x} + \bar{w}\frac{\partial \bar{\theta}}{\partial z} - \frac{\partial}{\partial x}\left(K_x^h \frac{\partial \bar{\theta}}{\partial x}\right) - \frac{\partial}{\partial z}\left(K_z^h \frac{\partial \bar{\theta}}{\partial z}\right) = 0, \tag{8}$$

Continuity:
$$\frac{\partial \bar{u}}{\partial x} + \frac{\partial \bar{w}}{\partial z} = 0, \tag{9}$$

where $\bar{u}$, $\bar{v}$, and $\bar{w}$ are, respectively, the x, y, and z components of velocity; $\bar{\theta}$ is the mean departure of the potential temperature from the neutral basic state; T and p are temperature and pressure, the basic state surface values of which are given by T_0 ($=\Theta$) and p_0; $\bar{\pi}$ is the mean departure of the Exner function, $\pi = c_p(p/p_0)^{R/c_p}$ from the basic state, π_0; f, g, c_p, and R are, respectively, the Coriolis parameter, gravitational acceleration, specific heat capacity at constant pressure, and specific gas constant; U_g and V_g are the x and y components of the geostrophic wind (imposed wind speed at the top of the model); K_x^m, K_z^m, K_x^h, and K_z^h are the horizontal and vertical diffusivities for momentum and heat. Gradients of synoptic-scale Exner function have been replaced by $-fV_g$ and fU_g in (5) and (6), respectively. For 1-D simulations, it is assumed that all derivatives with respect to x are zero.

The turbulent diffusivities K_z^m and K_z^h are parameterized by a cubic function of z, as suggested by O'Brien [9], such that the value and slope of the K-profile are matched to the expected linear behavior in the surface layer, and K asymptotically approaches some small value at the top of the boundary layer (typically 500–1500 m).

3.1. *Neutral Flow*

We have 1-D simulations of neutral flow in the lowest 1500 m achieved by using a low-resolution (9-element) domain and a high-resolution (17-element) domain, where most of the resolution increase is in the lowest 15 m. For each resolution, we compared results with and without the new log-linear boundary element. For this set of experiments the full equations (with Coriolis force and parameterized turbulence) are used. Figures 3a and b show, respectively, the x and y components of velocity. The high-resolution simulations with and without the log-linear boundary element

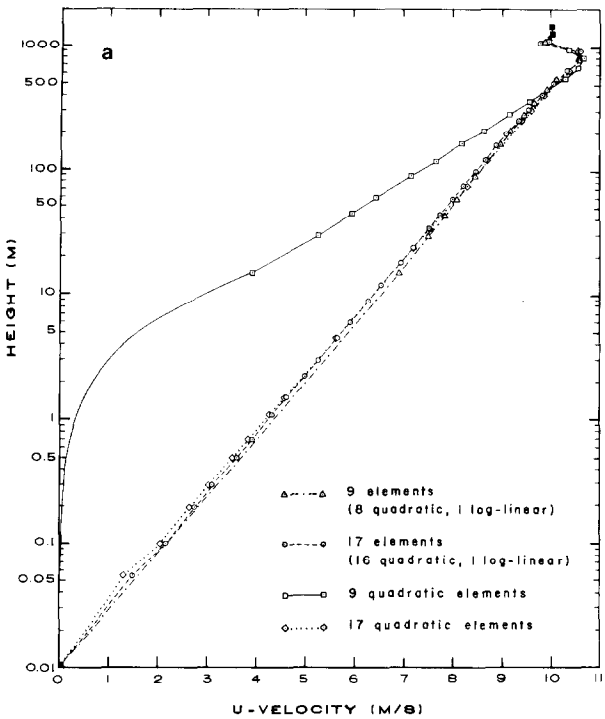

FIG. 3a. Calculations of the x component of velocity as a function of height resulting from a high-resolution (17 element) and two low-resolution (9 element) domains for an isothermal atmosphere.

gave nearly identical results. The low-resolution results show distinctly different behavior, however, when the log-linear boundary element is used. Whereas the fully quadratic model gives large errors extending to 500 m, the model using the log-linear boundary element is nearly indistinguishable from the high-resolution simulations.

3.2. *Nonneutral Flow*

We have further used the model to study influence on the flow produced by cooling at the earth's surface. For these experiments we used the log-linear functions to interpolate temperature as well as x and y components of velocity. We have used the results of Fig. 3 as initial conditions and have allowed the lower surface to cool at the rate of 1°C/h for 10 h. The results are shown in Figs. 4a and b for velocity and 4c for temperature. The surface cooling reduces the turbulent coupling between adjacent layers in the vertical direction, leading to larger velocity gradients. As the velocity profile adjusts, the localized region of enhanced wind speed (known as the "nocturnal jet") develops at 200–300 m. This jet is regularly observed [10, 11] and has

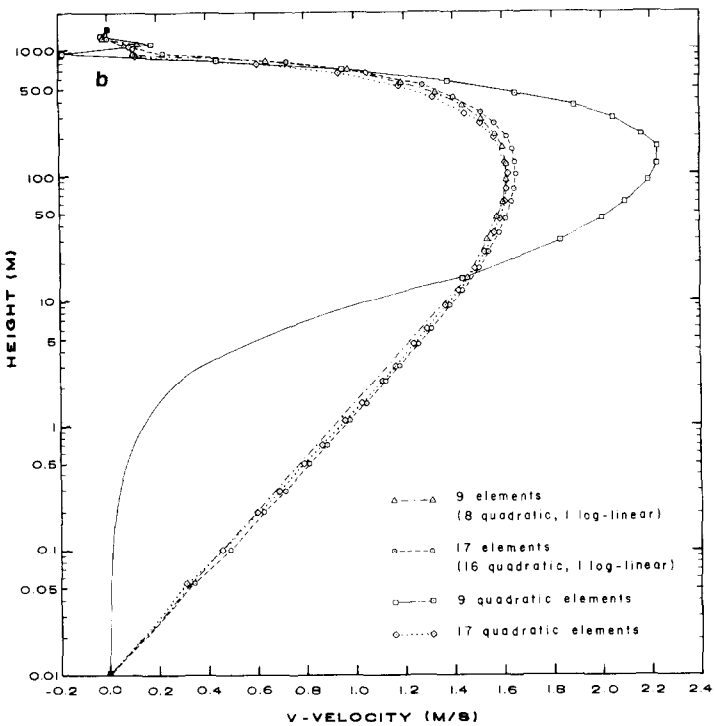

FIG. 3b. Calculation of the y component of velocity as a function of height resulting from a high-resolution (17 element) and two low-resolution (9 element) domains for an isothermal atmosphere.

magnitude that is influenced by the effects of baroclinity and terrain slope (features not included in the model from which our results were derived). Although its magnitude is somethat lower, the jet that develops in our model occurs at the generally expected height. Our turbulence parameterization in the upper part of the model is quite crude, so detailed comparisons with observations in that region would not be expected to show close correspondence. The purpose of this report is to examine the characteristics of the boundary element (where the turbulence is represented more accurately) when the log-linear interpolation is used.

Quadratic interpolation of velocities (Figs. 4a and b) in the low resolution model again is observed to be inadequate, whereas a low resolution with a log-linear boundary element performs quite well. In the interpolation of temperature, the log-linear boundary element shows significant improvement over quadratic interpolation for comparable resolution, but in this case, even the log-linear boundary element poorly represents the temperatures. Errors (relative to the high-resolution results) are decreased by about a factor of 2 when an additional element (10-element domain with log-linear boundary element) is added.

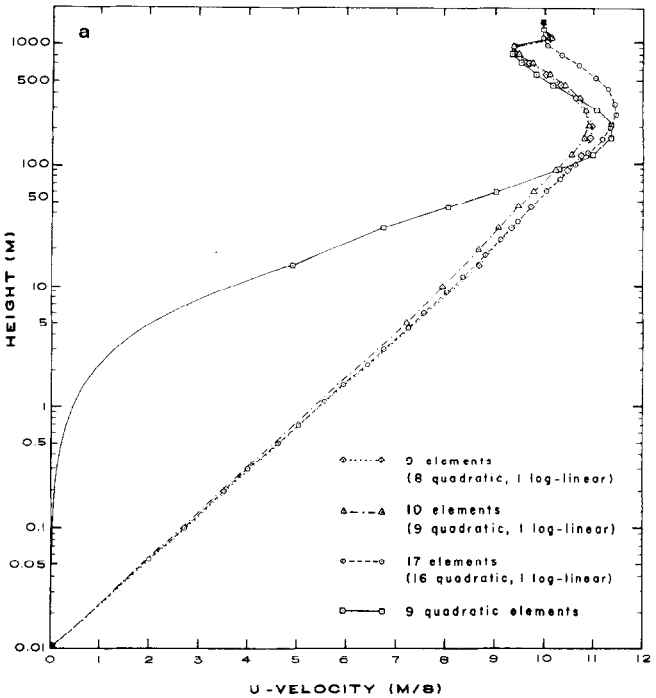

FIG. 4a. Calculation of the x component of velocity as a function of height resulting from a high-resolution (17 element) and three low-resolution (9 or 10 element) domains after 10 h of surface cooling at a constant rate of 1°C/h.

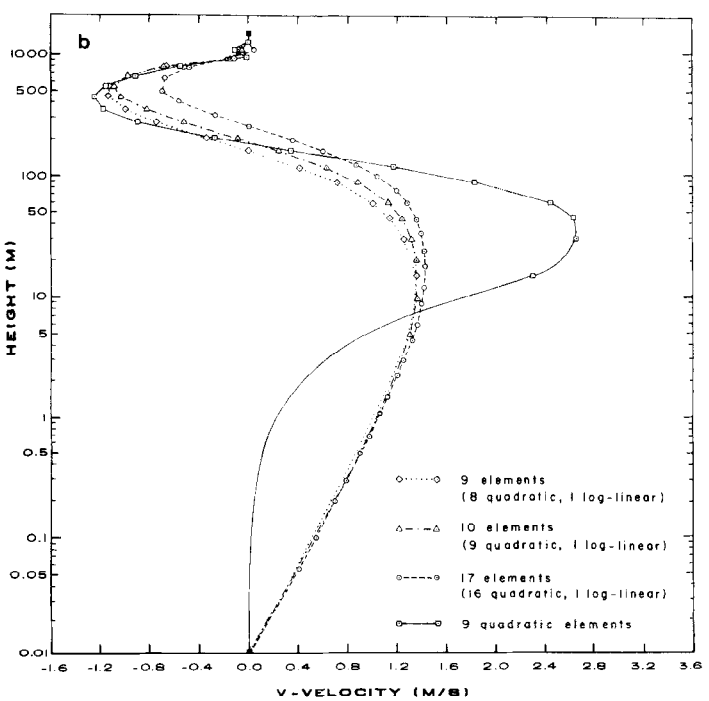

FIG. 4b. Calculation of the y component of velocity as a function of height resulting from a high-resolution (17 element) and three low-resolution (9 or 10 element) domains after 10 h of surface cooling at a constant rate of 1°C/h.

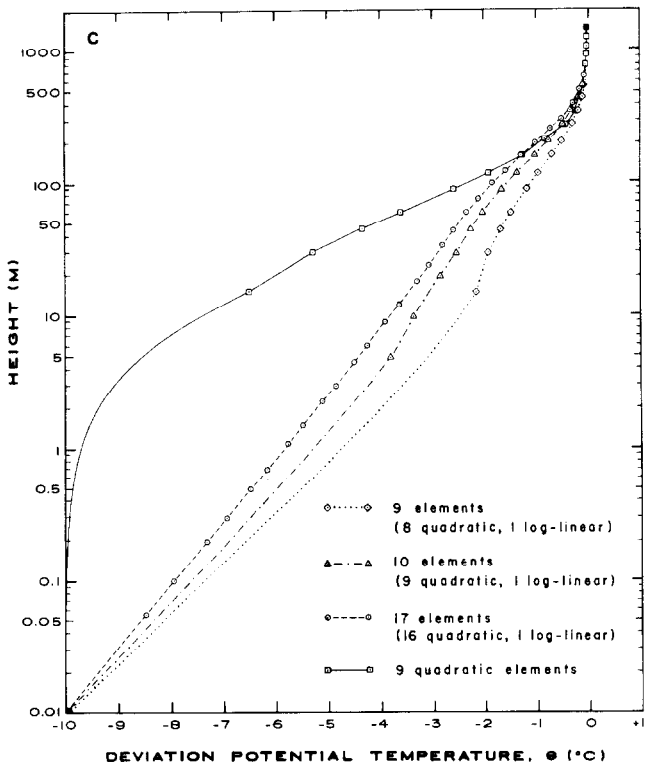

FIG. 4c. Calculation of the potential temperature as a function of height resulting from a high-resolution (17 element) and three low-resolution (9 or 10 element) domains after 10 h of surface cooling at a constant rate of 1°C/h.

4. CONCLUSIONS

We have developed a log-linear boundary element that has advantages over the conventional linear and quadratic elements for modeling flow near a boundary. Preliminary tests suggest that the advantages of this element are that fewer nodes are needed to resolve the logarithmic layer and that larger time steps can be employed without reduction of accuracy.

Application of the special element to a surface-cooling situation shows that both velocity and temperature are simulated better with the new element than with the conventional quadratic element. The log-linear interpolation seems somewhat more accurate for velocity than for temperature. This possibly is due to the shrinking of the vertical extent of the surface-based layer in which the temperature is truly log-linear. The decrease in size of the boundary element from 30 to 10 m, as shown in Fig. 4c, significantly reduces the interpolation error for temperature. These results suggest

that if temperature is to be modeled as accurately as velocity for nonneutral flows, greater resolution will be required near the boundary than is necessary for neutral flows.

APPENDIX: LOG-LINEAR/QUADRATIC SHAPE FUNCTIONS (ϕ_i) FOR USE IN BOUNDARY ELEMENTS

$$\phi_1 = A\left\{(\xi^2 - \xi)\left[-\ln\left(\frac{1+\Delta+\eta}{\Delta}\right) + \eta L2 + (1-\eta)L1\right]\right\},$$

$$\phi_2 = A\left\{(\xi^2 + \xi)\left[-\ln\left(\frac{1+\Delta+\eta}{\Delta}\right) + \eta L2 + (1-\eta)L1\right]\right\},$$

$$\phi_3 = A\left\{(\xi^2 + \xi)\left[-\ln\left(\frac{1+\Delta+\eta}{\Delta}\right) + (1+\eta)L1\right]\right\},$$

$$\phi_4 = A\left\{(\xi^2 - \xi)\left[-\ln\left(\frac{1+\Delta+\eta}{\Delta}\right) + (1+\eta)L1\right]\right\},$$

$$\phi_5 = A\left\{2(\xi^2 - 1)\left[\ln\left(\frac{1+\Delta+\eta}{\Delta}\right) - \eta L2 - (1-\eta)L1\right]\right\},$$

$$\phi_6 = A\left\{2(\xi^2 + \xi)\left[\ln\left(\frac{1+\Delta+\eta}{\Delta}\right) - \frac{1}{2}(1+\eta)L2\right]\right\},$$

$$\phi_7 = A\left\{2(\xi^2 - 1)\left[\ln\left(\frac{1+\Delta+\eta}{\Delta}\right) - (1+\eta)L1\right]\right\},$$

$$\phi_8 = A\left\{2(\xi^2 - \xi)\left[\ln\left(\frac{1+\Delta+\eta}{\Delta}\right) - \frac{1}{2}(1+\eta)L2\right]\right\},$$

$$\phi_9 = A\left\{2(\xi^2 - 1)\left[-2\ln\left(\frac{1+\Delta+\eta}{\Delta}\right) + (1+\eta)L2\right]\right\},$$

where $A = 1/2(2L1 - L2)$, $L1 = \ln((1+\Delta)/\Delta)$, $L2 = \ln((2+\Delta)/\Delta)$ and Δ is an adjustable parameter that depends on the ratio of the surface roughness to the physical height of the boundary element.

ACKNOWLEDGMENTS

This material is based upon work supported by the Division of Atmospheric Sciences, National Science Foundation, under Grant ATM 7923354. Acknowledgment is made to the National Center for Atmospheric Research, which is sponsored by the National Science Foundation, for computer resources used in this research.

REFERENCES

1. P. A. TAYLOR AND Y. DELAGE, *Boundary-Layer Meteorol.* **2** (1971), 108.
2. C. TAYLOR, T. G. HUGHES, AND K. MORGAN, *Comput Fluids* **5** (1977), 191.
3. A. G. HUTTON, *Appl. Math. Modelling* **3** (1979), 322.
4. A. G. HUTTON AND R. M. SMITH, On the finite element simulation of incompressible turbulent flow in general two-dimensional geometries, *in* "Numerical Methods in Laminar and Turbulent Flow" (Taylor and Schrefler, Eqs.), p. 229, Pineridge, Swansea, 1981.
5. J. A. BUSINGER, Turbulent transfer in the atmospheric surface layer, *in* "Workshop on Micrometeorology" (D. Haugen, Ed.), p. 67, Amer. Meteorol. Soc., Boston, 1973.
6. E. S. TAKLE, R. L. SANI, AND L. P. CHANG, A diabatic, turbulent, atmospheric boundary-layer model, in "Finite Elements in Fluids," Vol. 4, p. 347, Wiley, New York, 1982.
7. O. C. ZIENKIEWICZ, "The Finite Element Method," 3rd ed., p. 194, McGraw–Hill, London/New York, 1977.
8. S. CHAN, P. M. GRESHO, AND R. L. LEE, *Appl. Math. Modelling* **3** (1980), 335.
9. J. J. O'BRIEN, *J. Atmos. Sci.* **27** (1970), 1213.
10. A. J. THORPE AND T. H. GUYMER, *Q. J. Roy. Meteorol. Soc.* **103** (1977), 633.
11. L. MAHRT, *Q. J. Roy. Meteorol. Soc.* **107** (1981), 329.

RECEIVED: October 6, 1982; REVISED: August 24, 1983

E. S. TAKLE

Departments of Agronomy and Earth Sciences, Iowa State University, Ames, Iowa 50011

J. M. LEONE, JR.

Lawrence Livermore Laboratory, Livermore, California 94550